

# Splicing-related catalysis by protein-free snRNAs

Saba Valadkhan & James L. Manley

Department of Biological Sciences, Sherman Fairchild Center of Life Sciences, Columbia University, New York, New York 10027, USA

**Removal of intervening sequences from eukaryotic messenger RNA precursors is carried out by the spliceosome, a complex assembly of five small nuclear RNAs (snRNAs) and a large number of proteins. Although it has been suggested that the spliceosome might be an RNA enzyme, direct evidence for this has been lacking, and the identity of the catalytic domain of the spliceosome is unknown. Here we show that a protein-free complex of two snRNAs, U2 and U6, can bind and position a small RNA containing the sequence of the intron branch site, and activate the branch adenosine to attack a catalytically critical domain of U6 in a reaction that is related to the first step of splicing. Our data provide direct evidence for the catalytic potential of spliceosomal snRNAs.**

An essential step in the maturation of eukaryotic pre-mRNA is the removal of intervening sequences (introns) from the coding sequences (exons). The spliceosome—a dynamic assembly of five snRNAs and a large number of proteins—catalyses intron removal, or splicing, through two consecutive transesterification reactions<sup>1,2</sup>. In the first step, the 2'OH group of a conserved adenosine residue, bulged from an RNA–RNA duplex, is activated to attack the phosphodiester bond at the 5' splice site, resulting in the formation of a branched (lariat) intron containing a 2' to 5' phosphodiester bond and release of the 5' exon. The second step involves a nucleophilic attack by the 3'OH of the 5' exon on the phosphodiester bond at the 3' splice site, resulting in ligation of the two exons and excision of the intron lariat. Complementation studies *in vivo* and *in vitro* in addition to fundamental similarities to self-splicing group II introns<sup>3–8</sup> have suggested that the spliceosome might be an RNA enzyme. Of the five spliceosomal snRNAs, U2 (which base-pairs with the intron branch site) and U6 (which interacts with the 5' splice site) are the only ones required for both steps of splicing<sup>9,10</sup>, and mutagenesis studies support possible roles in catalysis for these two RNAs<sup>11–17</sup>. However, the ability of these RNAs and/or spliceosomal proteins<sup>18,19</sup> to participate directly in catalysis has not been demonstrated. Previous studies that investigated the possible catalytic activity of snRNAs used *in vitro* evolution and selection<sup>20,21</sup> and isolated U6 and/or U2-derived ribozymes that catalysed reactions not closely related to the mRNA splicing reactions.

We have previously shown that U2 and U6 snRNAs can form a base-paired complex in the absence of proteins that closely resembles the complex thought to exist in the active spliceosome, and we also provided evidence for the presence of a genetically proven tertiary interaction<sup>22</sup> in this complex (Fig. 1, ref. 23, and S.V. and J.L.M., unpublished data). We show here that this complex can bind and position a short RNA oligonucleotide that contains the branch consensus sequence, and catalyses a reaction in which the 2'OH group of a bulged adenosine attacks a specific phosphodiester bond in U6, resulting in the formation of an unusual phosphotriester bond. The sequence and ionic requirements for this reaction closely resemble those of authentic splicing. Our data provide evidence for the ability of spliceosomal snRNAs to function as the catalytic domain of the spliceosome.

## Catalytic activity of the U2–U6 complex

To assay the possible catalytic activity of spliceosomal snRNAs in the absence of proteins, we incubated a previously characterized U2–U6 snRNA complex, consisting of *in vitro* transcribed and purified

segments of human U2 and U6 snRNAs<sup>23</sup>, with radiolabelled short RNA oligonucleotides that contained the consensus branch site sequence (the branch oligonucleotide (Br), Fig. 1) or the 5' splice-site consensus sequence under various ionic, temperature and pH conditions. Although no significant reaction was observed with the 5' splice site oligonucleotide, in the presence of Mg<sup>2+</sup> and after 24 h incubation at room temperature about 0.1% of Br was converted to a new, low-mobility RNA species on denaturing polyacrylamide gel electrophoresis (PAGE) (Fig. 2a). Formation of this product (RNA X) was dependent on the presence of both U2 and U6 in the reaction, and was greatly reduced after incubation on ice or at temperatures close to the melting temperature (*T*<sub>m</sub>) of the U2–U6 complex (not shown). RNA X accumulated linearly for at least 2 h and continued to increase for nearly 20 h (Fig. 2b). Varying the concentration of Br or the U2–U6 complex over a wide range resulted in roughly linear increases in the formation of RNA X, followed by a plateau at higher concentrations (Fig. 2c and data not shown), with an apparent Michaelis constant (*K*<sub>m</sub>) of 5 μM and a reaction rate (*k*<sub>obs</sub>) of 0.002 min<sup>-1</sup> under standard reaction conditions. To prove that RNA X indeed resulted from a new covalent linkage and not an unusually strong non-covalent interaction, purified RNA X was denatured at 90 °C for 5 min in 9 M urea plus

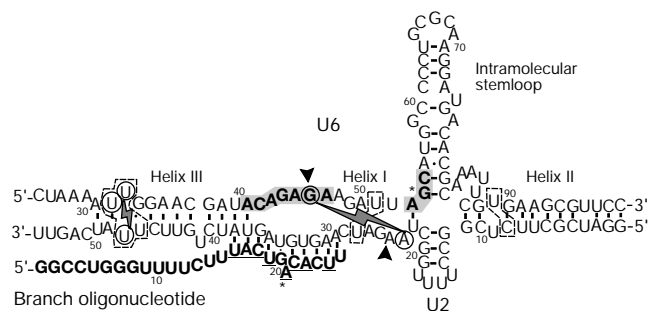


**Figure 1** Base-pairing interactions in the *in vitro*-assembled complex of U2–U6 and the branch oligonucleotide (Br). Shaded boxes mark the invariant regions in U6 and previously established base-paired regions are indicated. Dashed lines connect psoralen-crosslinkable nucleotides (S.V. and J.L.M., unpublished data). The circled residues connected by a zigzag can be crosslinked by ultraviolet light. The underlined residues in Br constitute the yeast branch consensus sequence. Asterisks denote the residues involved in the covalent link between Br and U6 in RNA X (see text). Arrowheads point to residues involved in a genetically proven interaction in yeast<sup>22</sup>. Numbers indicate nucleotide positions from the 5' ends of full-length human U2 and U6.

12 mM EDTA, rapidly cooled and loaded on a gel containing 8 M urea and 40% formamide. No detectable dissociation was observed (Fig. 2d). Notably, RNA X showed anomalous mobility on 8% and 16% denaturing gels compared with RNA markers of known length, which is a property indicative of nonlinear RNA species (Fig. 2e).

We next tested the ionic requirements for the formation of RNA X (Fig. 2f and data not shown). RNA X formed with the same efficiency in buffers that contained HEPES, MOPS or sodium cacodylate instead of Tris. Increasing the Mg<sup>2+</sup> concentration from 10 to 200 mM had a modest effect on RNA X formation, whereas RNA X did not form in the absence of divalent cations or in the presence of 0.4 M NaCl, which fully supports the formation of the annealed U2–U6 complex<sup>23</sup>. Notably, RNA X did not form with Mn<sup>2+</sup> as the only divalent cation in the buffer. Indeed, addition of Ca<sup>2+</sup>, Mn<sup>2+</sup> or ammonium salts to Mg<sup>2+</sup> reduced the efficiency of RNA X formation, although Ca<sup>2+</sup> alone weakly supported product formation.

### The bulged adenosine in Br attacks the AGC triad of U6

To determine the constituents of RNA X, reactions were performed with 5' or 3' end-labelled U2, U6 or Br. Label at either end of U6 or Br, but not U2, appeared in RNA X (not shown). These observations, which are consistent with an RNase T1 fingerprint of 5' end-labelled RNA X (not shown) and with results from alkali treatment of the product (see below), indicate the presence of full-length U6 and Br, but not U2, in RNA X. Dephosphorylation of the 5' end or introduction of a cyclic phosphate at the 3' end of U6 or Br did not affect the rate of RNA X formation (not shown), indicating that the 5' and 3' ends of U6 and Br are not involved in the new covalent bond in RNA X. These results suggest that RNA X is probably an X-shaped molecule.

To map the location in U6 of the covalent bond between U6 and Br, purified RNA X was annealed to an oligonucleotide that was complementary to the 3' end of U6 (nucleotides 81–99) and subjected to reverse transcription. Notably, a strong stop immediately 3' to A53, with a minor stop 5' to that residue, was observed (Fig. 3a). This is significant because A53 lies within the so-called AGC triad, which is one of two invariant, functionally critical regions of U6 (refs 1, 2, 11–14), and which is also conserved in U6atac (the U6 counterpart in the ATAC spliceosome)<sup>1,24,25</sup>. Base or backbone mutations in this region can be frequently incompatible with splicing<sup>11–17</sup>. A similarly positioned AGC triad in domain 5 of

self-splicing group II introns is thought to be part of the active site of that ribozyme<sup>1,5</sup>.

We next used limited enzymatic digestion with RNase T2 (Fig. 3b), T1 (Fig. 3c) and P1 (not shown) of purified RNA X labelled at the 5' end of Br to map the location of the linkage in Br. Whereas scission of phosphodiester bonds up to G20 resulted in release of 5' fragments of Br, fragments resulting from digestion after A21 were absent (Fig. 3b, c and data not shown), suggesting that this residue is involved in the covalent linkage between U6 and Br (see below). The results obtained from Br point mutants that contained RNase T1 digestion sites close to A21 (Br C18G, Br U19G and Br A23G, which have at most small effects on catalysis; see below) confirmed the data from wild-type Br (Fig. 3c and data not shown). The above data also rule out the possibility that RNA X is a hyperstable, non-covalent complex by demonstrating its accessibility to RNases (and iodoethanol cleavage; see below) throughout its length. Taken together, the mapping data are consistent with the hypothesis that RNA X is X-shaped, with U6 and Br joined covalently through residue A53 in the conserved AGC triad in U6 and the bulged A (A21; see below) in Br.

### A phosphotriester linkage between U6 and Br

We next wished to characterize the nature of the linkage between U6 and Br in RNA X. We first subjected internally labelled RNA X to complete RNase P1 or T2 digestion, but were unable to isolate a nuclease-resistant core (data not shown). This indicates that the covalent bond between U6 and Br can either be digested by these enzymes or is susceptible to hydrolysis mediated by solvent exposure after complete digestion (see below). In any event, we required alternative methods to characterize the U6–Br linkage.

Treatment of phosphorothioate-substituted RNA with iodoethanol results in specific backbone cleavage at sites of phosphorothioate substitutions, and can thus be used to map sites of interaction or interference that prevent cleavage<sup>26</sup>. We therefore used iodoethanol cleavage with 5' and 3' end-labelled RNA X prepared from phosphorothioate-substituted U6, in which each U6 contained, on average, one randomly distributed phosphorothioate linkage<sup>27</sup> (see Methods). The iodoethanol cleavage patterns confirmed the reverse transcription mapping data and, more importantly, localized the site of covalent bond formation to the backbone phosphate between A53 and G54 (Fig. 4a). In  $\alpha$ -S-GTP-substituted U6 RNA, the iodoethanol cleavage ladders stopped at G54 with both 5'- and

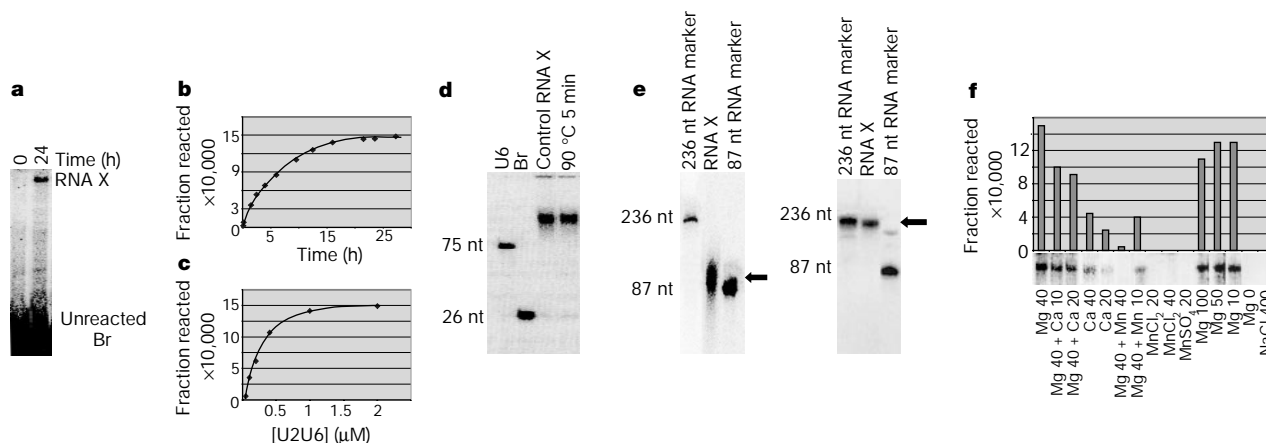


**Figure 2** Characterization of RNA X. **a**, Formation of RNA X. Reaction products were resolved by denaturing PAGE, and the gel is shown from the level of the wells to the bottom. **b**, Time course of formation of RNA X. **c**, RNA X formation as a function of U2–U6 complex concentration [U2U6]. **d**, Resistance to denaturation. Control RNA X, RNA X after two gel-purification steps, before stringent denaturation. The denaturation condition is indicated above the far right lane. Gel composition: 16% PAGE, 8 M urea and 40%

formamide. Sizes of U6 and Br are indicated. nt, nucleotide. **e**, Anomalous gel mobility of RNA X. The arrows point to the location of RNA X. Gel composition: 8% (left) and 16% (right) denaturing PAGE. **f**, Cationic requirements for formation of RNA X. The concentration of cations in each reaction (in mM) is indicated below each lane. Efficiency of RNA X formation was quantified by PhosphorImager and plotted.

3'-labelled U6 (Fig. 4a, left and right panels, respectively). This contrasted with results obtained from iodoethanol cleavage of phosphorothioate substitution at other sites (Fig. 4a) and with other  $\alpha$ -S-nucleoside 5'-triphosphate (NTP) substitutions (for example, Fig. 4b) in which one of the two U6 fragments remained attached to Br, and thus was not detected at its normal location. For example, cleavage of the phosphorothioate bond 5' of G49 resulted in a U6 25–48 fragment that is released from RNA X (Fig. 4a, left panel) and a U6 49–95 fragment that stays attached to Br and

therefore has a much slower mobility—such that it was not resolved on the gels (Fig. 4a, right panel)—compared with the U6 49–95 fragment in the control lane. The unusual iodoethanol cleavage pattern with G54 phosphorothioate substitution can be explained if the link between U6 and Br is such that iodoethanol cleavage at the phosphorothioate 5' of G54 would break U6 in two halves such that either half of U6 can be released from RNA X, that is, if the link between U6 and Br in RNA X is on the phosphorus atom (Fig. 4c). Indeed, the reaction of iodoethanol with a phosphorothioate triester results in release of either of the three phosphate ligands<sup>28</sup>. A covalent bond originating on a sugar or a base in U6 would have resulted in an iodoethanol cleavage pattern in which one of the two U6 halves would remain attached to Br. Involvement of backbone functionalities as reacting groups in RNA X is consistent with the mild phenotype of U6 mutations in the AGC region (see below).

To extend this analysis, we took advantage of the alkali sensitivity of RNA X (half-life in pH 12 at 50 °C: <3.5 min). Purified RNA X labelled at the 5' end of U6 or Br was treated with alkali (pH 12, 20 min at room temperature) and compared with similarly labelled U6 or Br. These conditions resulted in partial conversion of RNA X to full-length U6 and Br without significant backbone phosphodiester breaks, confirming that the chemical bond formed in the product is unusually alkali-sensitive (Fig. 4d, lane 1). No difference in mobility of released U6 and Br compared with unreacted controls could be observed, even after long electrophoresis times (not shown). In addition, alkali hydrolysis of U6 and Br released from RNA X resulted in fragments with identical mobilities to those of controls (Fig. 4d, compare lanes 4 and 7 with 5 and 6), even though a difference in relative molecular mass of less than 40 could have been detected (for example, compare the two hydrolysis ladders in Fig. 3c). As formation of an adduct between U6 and Br without a leaving group is entropically unfavourable, the above results are consistent with a very small leaving group, such as H<sub>2</sub>O. Taken together, the alkali sensitivity of RNA X and the phosphorothioate substitution data are consistent with a phosphotriester linkage between U6 and Br in RNA X, with the phosphate bond between A53 and G54 forming the triester.

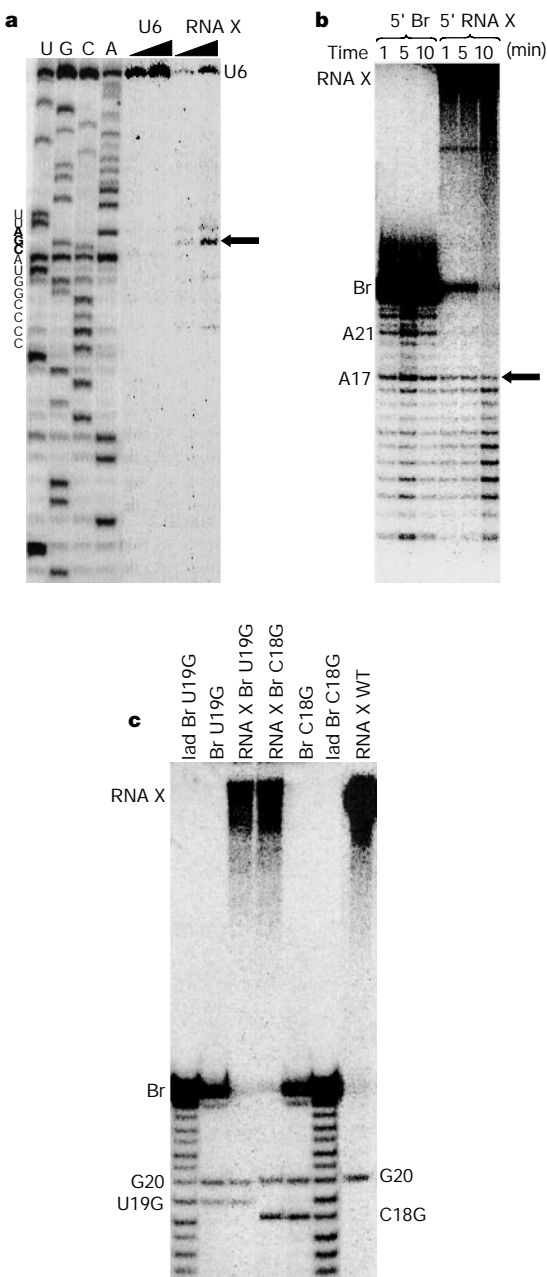


**Figure 3** Mapping the site of the covalent linkage in RNA X. **a**, Reverse transcription mapping of the site of the covalent link in U6. Lanes marked U, G, C and A are sequencing reactions. Reverse transcription of two concentrations of U6 and RNA X are presented. The arrow points to the site of the strongest stop. A partial sequence of U6 is indicated to the left of the panel, with the AGC triad in bold letters. **b**, Limited RNase T2 digestion of RNA X labelled at the 5' end of Br. Times of T2 digestion are indicated. The arrow points to the site of stop in the ladder. **c**, Mapping the site of the covalent link on Br by limited RNase T1 digestion of RNA X that was 5'-labelled on Br. The identity of the Br derivative used is indicated above each lane. Lad, alkaline hydrolysis ladder; WT, wild type.

### Sequence requirements for RNA X formation

We next examined the effects of mutations in Br and U6 on RNA X formation (Fig. 5). Mutations that disrupted the base-pairing interaction between U2 and Br (Fig. 5a, transversion mutation) or that changed the base identity of A21 (A21 to G or C) resulted in marked decreases in the formation of RNA X. Mutations that removed the bulged residue in Br (deletion of A21 or G20) or disrupted U2–U6 helix III by competing with U6 for base-pairing to U2 in this region (Fig. 5a, 5'-complementary mutant) had the most marked phenotype, reducing the rate of RNA X formation essentially to zero. Point mutations in other positions or removal of residues 1–14 of Br had modest effects on the formation of RNA X (Fig. 5a and not shown). Notably, mutations in the ACAGAGA box of U6 (Fig. 5b; see also Fig. 1)—one of the two invariant, functionally critical regions of U6 (refs 1, 2, 11–14, 16, 17)—resulted in loss of catalytic activity, although mutations in the AGC triad had only mild effects. The discrepancy between the modest effect of AGC mutants in our system and stronger phenotypes seen in some cases *in vivo*<sup>11–15</sup> might reflect a role for the AGC triad other than 2'OH positioning and activation, for example, a function in 5' splice-site coordination. Alternatively, different steps might be rate limiting in the two systems.

All Br mutants were also tested for binding to the U2–U6 complex (see Methods) to distinguish between binding versus catalytic defects. As expected, deletion of Br A21 or G20 and the 5'-complementary mutation resulted in significant increases in binding, whereas other Br mutations, with the exception of the transversion mutation, did not significantly affect binding (not shown). To determine whether the two mutations in the U6

ACAGAGA box interfered with binding or catalysis, we assayed Br binding directly and also tested the activity of the U6 mutants as a function of Br concentration. The results (not shown) indicate that both mutants were defective in catalysis, although the U6 44–47 UCUC mutation, which could enhance base pairing with U2 and

hence competition with Br (see Fig. 1), also decreased binding. Thus, in marked similarity to the splicing reaction, formation of RNA X requires an intact U2–U6–Br base-pairing interaction, the ACAGAG box in U6 and a bulged A.

We were able to partially suppress the loss of function resulting

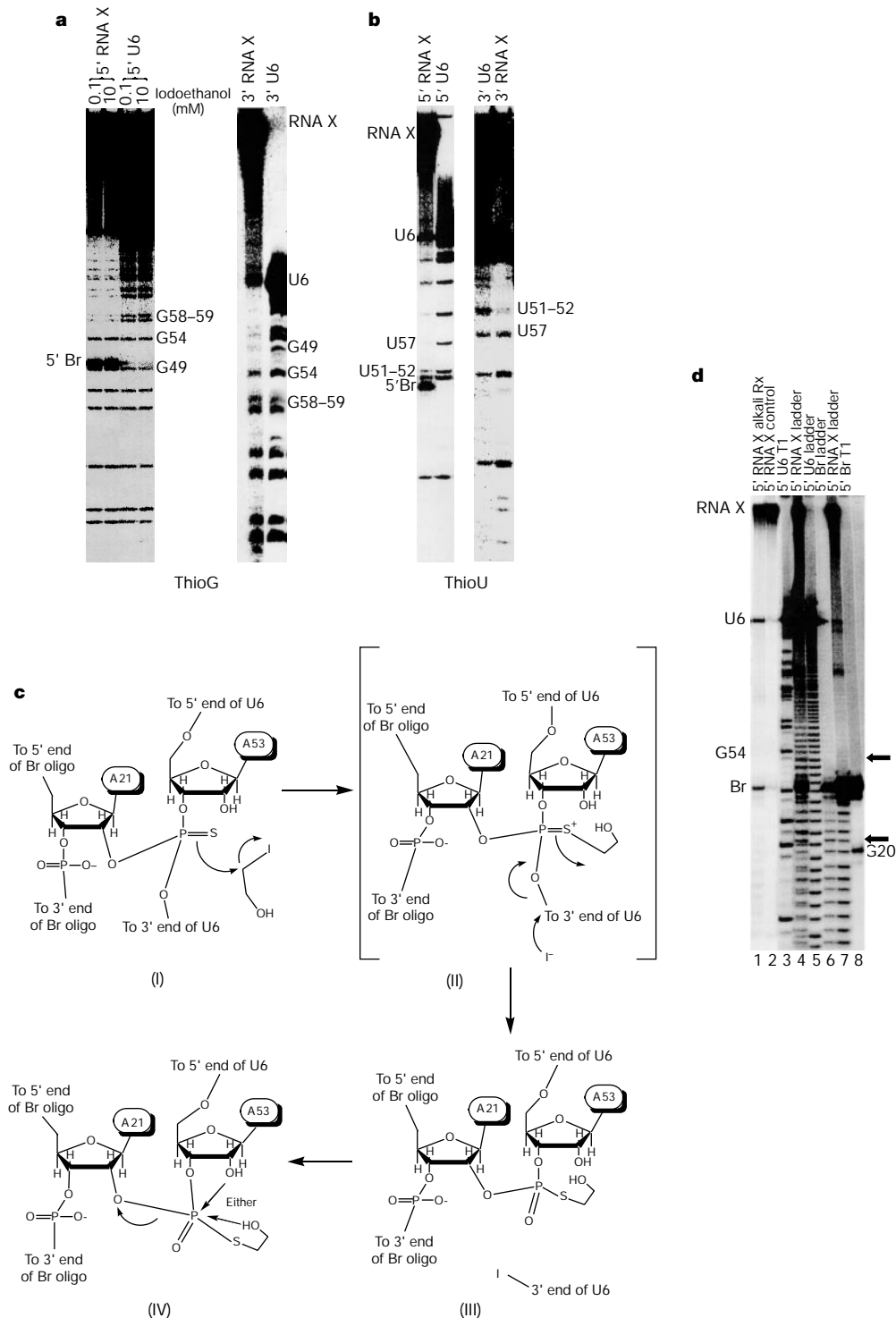
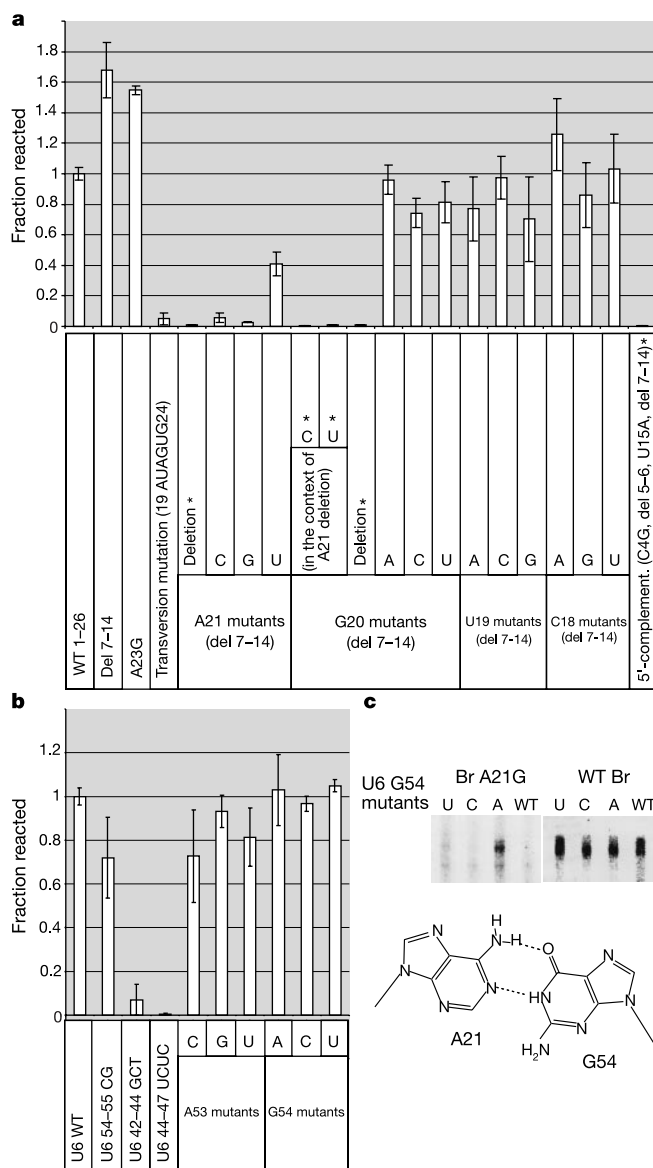


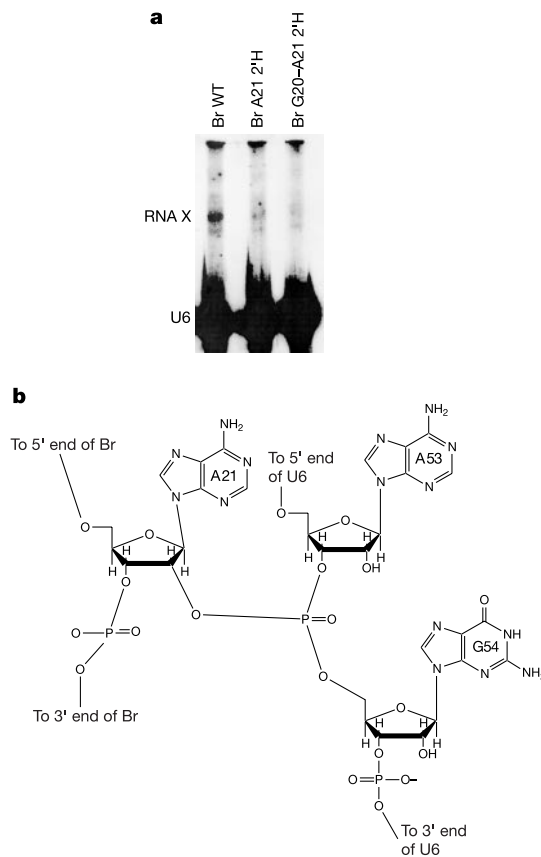
**Figure 4** Characterization of the new covalent bond. **a**, Iodoethanol treatment of 5'-labelled (left) and 3'-labelled (right) RNA X formed with  $\alpha$ -S-GTP. **b**, Iodoethanol treatment of 5'-labelled (left) and 3'-labelled (right) RNA X formed with  $\alpha$ -S-UTP. **c**, The iodoethanol cleavage pathway for the proposed phosphorothioate triester (adapted from ref. 28). Sulphur launches a nucleophilic attack on iodoethanol (I), resulting in alkylation of sulphur (II). In a concerted reaction, iodide ion reacts with either of the phosphorus ligands

(II). The resulting alkyl phosphorothioate (III) can further dissociate<sup>26</sup> after a nucleophilic attack on the phosphodiester by either the 2'-OH of A53 or the OH of the alkylated sulphur (IV). Oligo, oligonucleotide. **d**, Limited alkali hydrolysis of RNA X. T1, limited RNase T1 digestion reactions; ladder, limited alkali hydrolysis reactions; alkali Rx, mild alkali treatment reaction. Arrows point to the two nucleotides involved in the covalent bond between U6 and Br. 5'-labelled RNA X is labelled on both U6 and Br.

from the A21G mutation in Br by a compensatory mutation in U6 that changed G54 to A (Fig. 5c). This observation is consistent with a direct interaction between A21 and G54, probably as a symmetrical G–A mismatch<sup>29</sup> (Fig. 5c). This result further supports the mapping data in U6 and Br, and also shows that the strong effects of A21 mutations result from loss of a functionally important interaction and not the absence of a reacting group. The interaction might serve to recognize and/or position the bulged residue of Br in the catalytic centre. Notably, the functional groups involved in this type of G–A base pair, N1 and N6 of adenosine, have been implicated in branch recognition in the spliceosome<sup>30</sup>. A similar interaction might be one of the means by which the branch adenosine is recognized and positioned in the active site of the spliceosome.



We next investigated whether the 2'OH on the bulged A in Br (A21) participates in catalysis. A DNA oligonucleotide with identical sequence to Br was not active in RNA X formation (data not shown). Use of chemically synthesized Br with a single 2'H substitution at residue A21 (Br A21 2'H) resulted in a marked reduction in formation of RNA X, although low levels were still detected (Fig. 6a). In the spliceosome, the residue immediately 5' to the branch nucleotide (G20 here) can also assume a bulged conformation and serve as the nucleophile for the first step of splicing<sup>31</sup>, and this could be responsible for the residual RNA X formation. Alternatively, the small amount of product formed with Br A21 2'H could reflect a linkage between Br and U6 located elsewhere in the two molecules<sup>31</sup>. To distinguish between these two possibilities, we tested a Br derivative with 2'H at both A21 and G20 (Br G20–A21 2'H). Formation of RNA X with this double-substituted Br was nearly undetectable, even at very high Br concentrations (Fig. 6a). Although it cannot be ruled out that the effect of 2'H substitution at G20 reflects a general stimulatory effect of a 2'OH group at this position, these results support the idea that at least most of the low Br A21 2'H activity results from G20 functioning as the nucleophile. To rule out the possibility that the inactivity of the deoxyribonucleoside-substituted Br oligonucleotides resulted from a binding defect rather than a defect in chemistry, we tested them both for binding to the U2–U6 complex and for their ability to competitively inhibit the reaction of wild-type Br with the U2–U6 complex. Both Br derivatives behaved indistinguishably from wild-type Br in these assays (data not shown). Together with the mutagenesis and enzymatic mapping data, these results indicate that the 2'OH on



A21 participates directly in the covalent link between U6 and Br in RNA X (Fig. 6b).

### Discussion

Our data show that a protein-free, base-paired RNA complex containing fragments of U2 and U6 snRNAs can catalyse a novel reaction similar to the first step of splicing, which leads to the formation of an X-shaped product (RNA X). Our results indicate that RNA X contains a 2'OH-phosphoester bond similar to that observed in lariat splicing products, but with the difference that in RNA X the 5' end of the branch acceptor (U6) is not displaced, thereby creating an unusual phosphotriester. The 2'OH of U6 A53 is close to the triester linkage, providing an explanation for the alkali sensitivity of RNA X (see Fig. 6b). A large, branched RNA species such as RNA X is probably stabilized by extensive stacking interactions<sup>32</sup> and by cations that neutralize the negative charge repulsion in the compact branch core. It is plausible to think that a divalent cation, or another interaction, keeps the 2'OH of A53 protonated to prevent it from attacking the triester structure at neutral pH. The sensitivity of RNA X to complete digestion with RNases is consistent with a triester linkage, as the 2'OH on A53 can be activated to attack the triester, resulting in its dissociation to a diester, which can be further cleaved to nucleotides. The low efficiency of product formation can also be explained by the unusual chemistry, involving extraction of H<sub>2</sub>O rather than the 5' end of U6 providing the leaving group, which would have created a Y-like structure with a 2' to 5' linkage. It is noteworthy that in ligase reactions the ultimate leaving group is H<sub>2</sub>O, although the reaction involves multiple steps<sup>33</sup>. Formation of RNA X may also involve more than one step. Lack of a 5' splice-site acceptor in our system may place the non-bridging phosphate oxygen of G54 in the pocket intended for the leaving group, thereby promoting formation of the triester rather than a transesterification reaction.

Our data demonstrate the ability of protein-free spliceosomal snRNAs to catalyse a reaction related to the first step of splicing, with the 2'OH of a bulged A residue in a base-paired, intron-like RNA attacking the phosphate 5' to a G residue in the invariant AGC triad of U6. The strong similarities in the sequence requirements between this reaction and the first step of splicing indicate similarities in the active site of the two reactions, with the ACAGAG and the AGC invariant regions of U6 located in close proximity to the reacting groups and having important roles in the chemistry of a metal-dependent reaction in both systems. Aberrant splicing reactions in the spliceosome in which the backbone of U6, rather than the 5' splice site, is attacked by the branch A are not unprecedented<sup>34</sup>. Furthermore, the location of the covalent bond in U6 (3' of A53) is immediately adjacent to the site of an intron insertion in a fungal U6 gene, which is believed to have resulted from a faulty splicing reaction<sup>35</sup>. In any event, our data point to the competence of the spliceosomal U2 and U6 snRNAs to function as the catalytic active site for the first step of splicing, and provide direct evidence for RNA-based catalysis in the spliceosome. □

### Methods

#### Transcription and end labelling

U2 and U6 snRNA fragments were transcribed and the 5' ends were labelled as described<sup>23</sup>. Labelling of the 3' end was done according to published procedures<sup>36</sup>. Branch oligonucleotides were made by *in vitro* transcription (using a T7 transcript with extra nucleotides added at the 3' end for efficiency reasons, followed by DNazyme<sup>37</sup> removal of these extra nucleotides and gel purification) and by chemical synthesis (Dharmacon Biotech). We carried out end labelling as described for U2 and U6.

#### Catalytic assays

U2 and U6 were annealed as described<sup>23</sup> in a buffer containing 40 mM Tris, pH 7.2 and 40 mM MgCl<sub>2</sub>, at a final concentration of 2 μM, followed by the addition of Br at a final concentration of 10 nM in a typical reaction. Reaction mixtures were routinely incubated at room temperature for 24 h and were analysed by 12% or 20% denaturing PAGE. For

large-scale reactions, the concentration of Br was increased to 9 μM, and after incubation at room temperature for 24 h, RNA X was purified from a 12% denaturing gel. Reactions for 3' labelling were as described with oligonucleotides specific to U6 or Br<sup>36</sup>. The purified products were directly used in kinasin reactions for 5' labelling on Br. To obtain products that were 5'-labelled on U6, RNA X was dephosphorylated before the 5' labelling reaction, resulting in simultaneous labelling of the 5' ends of both U6 and Br, and repurified.

We carried out reverse transcription, RNase T1 and alkaline hydrolysis reactions as described<sup>23</sup>. To hydrolyse the link between U6 and Br in RNA X, alkali hydrolysis reactions<sup>23</sup> were done at room temperature for 20 min. RNase T2 (Gibco) reactions were done in a buffer containing 10 mM sodium citrate pH 5.0, 0.5 mM EDTA and 1.5 M urea at 55 °C for 2 min.

#### Phosphorothioate substitution studies

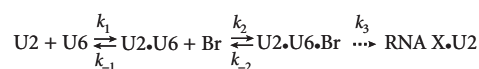
Transcription of U6 with α-thio-NTPs (Trilink Biotech and NEN) was done as described<sup>27</sup> so that each molecule would contain on average only a single thio group. Separate *in vitro* transcription reactions were set up for each α-S-NTP. The phosphorothioate-containing U6 was purified and treated with calf intestinal alkaline phosphatase to remove the 5' phosphate. Typical large-scale reactions were set up for each α-S-NTP-containing U6, and the resulting RNA X was gel-purified and labelled at the 5' end, resulting in labelling of both U6 and Br. Labelling of the 3' end of thio-U6-containing RNA X was done as described above, using a U6-specific oligonucleotide. Iodoethanol cleavage of the phosphorothioate-containing RNA X was done as described<sup>27</sup> and the reactions were loaded directly onto a 20% denaturing gel, along with identical reactions with similarly labelled U6 as a control.

#### Mutagenesis and binding studies

For mutagenesis studies, for each mutant the amount of RNA X formed was measured under standard reaction conditions in at least three independent experiments, and the average of normalized values was plotted as a fraction of wild type with two standard deviations as the error bars. For Br-binding studies, reactions were allowed to proceed for 2 h, after which they were divided in two; half was loaded on a denaturing 12% gel and the other half was loaded on a non-denaturing 8% PAGE run at 4 °C, followed by quantification of the reacted, bound and unbound Br. The bound and reacted fractions were normalized to the total amount of Br in each lane. As the bound Br on native gels also contained the reacted fraction, the amount of unreacted bound fraction was calculated by subtracting the reacted fraction from it. To test the ability of Br derivatives to competitively inhibit wild-type Br, 1–10 μM of the Br species to be tested was added to a typical reaction containing labelled wild-type Br and U6–U2 complex. The quantity of labelled RNA X formed was then compared with similar reactions containing the same concentration of unlabelled wild-type Br. All quantifications were done using a Molecular Dynamics PhosphorImager, with the amount of RNA X normalized to the amount of input in each reaction.

#### Kinetics

To determine the reaction rate ( $k_{obs}$ ) the natural log of substrate remaining (1 – fraction RNA X/fraction RNA X at the end point of the reaction) was plotted against time under standard conditions, and the slope of the line was calculated to determine  $k_{obs}$ . For those Br mutants that showed significant increases in binding to the U2–U6 complex, the catalytic constant,  $k_{cat}$ , of the reaction was determined. The amount of RNA X was measured after 2 h of reaction with a U2–U6 complex concentration of 0.1 μM and different concentrations of the branch oligonucleotide (10 nM to 50 μM), and the apparent  $K_m$  and  $V_{max}$  (velocity of enzyme-catalysed reaction at infinite concentration of substrate) of the reactions were determined by plotting the data on an Eisenthal–Cornish-Bowden plot. The value for  $k_{cat}$  was calculated as  $V_{max} /$  the concentration of the U2–U6 complex, [U2U6]. The reaction was assumed to proceed according to the equation (dots represent non-covalent binding)



Received 19 June; accepted 10 August 2001.

- Nilsen, T. W. In *RNA Structure and Function* (eds Simons, R. & Grunberg-Manago, M.) 279–307 (Cold Spring Harbor Laboratory Press, Cold Spring Harbor, New York, 1998).
- Burge, C. B., Tuschl, T. H. & Sharp, P. A. In *RNA World II* (eds Gesteland, R. F., Cech, T. R. & Atkins, J. E.) 525–560 (Cold Spring Harbor Laboratory Press, Cold Spring Harbor, New York, 1998).
- Hetzler, M., Wurtzer, G., Schweyen, R. J. & Mueller, M. W. Trans-activation of group II intron splicing by nuclear U5 snRNA. *Nature* **386**, 417–420 (1997).
- Collins, C. A. & Guthrie, C. The question remains: is the spliceosome a ribozyme? *Nature Struct. Biol.* **7**, 850–854 (2000).
- Newman, A. RNA splicing: out of the loop. *Curr. Biol.* **7**, R418–R420 (1997).
- Yean, S. L., Wuenschell, G., Termini, J. & Lin, R. J. Metal-ion coordination by U6 small nuclear RNA contributes to catalysis in the spliceosome. *Nature* **408**, 881–884 (2000).
- Sontheimer, E. J., Sun, S. & Piccirilli, J. A. Metal ion catalysis during splicing of pre-messenger RNA. *Nature* **388**, 801–805 (1997).
- Gordon, P. M., Sontheimer, E. J. & Piccirilli, J. A. Metal ion catalysis during the exon-ligation step of nuclear pre-mRNA splicing: extending the parallels between the spliceosome and group II introns. *RNA* **6**, 199–205 (2000).
- O'Keefe, R. T., Norman, C. & Newman, A. J. The invariant U5 snRNA loop 1 sequence is dispensable for the first catalytic step of pre-mRNA splicing in yeast. *Cell* **86**, 679–689 (1996).

10. Segault, V. *et al.* Conserved loop I of U5 small nuclear RNA is dispensable for both catalytic steps of pre-mRNA splicing in HeLa nuclear extracts. *Mol. Cell. Biol.* **19**, 2782–2790 (1999).
11. Fabrizio, P. & Abelson, J. Two domains of yeast U6 small nuclear RNA required for both steps of nuclear precursor messenger RNA splicing. *Science* **250**, 404–409 (1990).
12. Madhani, H. D., Bordonne, R. & Guthrie, C. Multiple roles for U6 snRNA in the splicing pathway. *Genes Dev.* **4**, 2264–2277 (1990).
13. Datta, B. & Weiner, A. M. The phylogenetically invariant ACAGAGA and AGC sequences of U6 small nuclear RNA are more tolerant of mutation in human cells than in *Saccharomyces cerevisiae*. *Mol. Cell. Biol.* **13**, 5377–5382 (1993).
14. Wolff, T., Menssen, R., Hammel, J. & Bindereif, A. Splicing function of mammalian U6 small nuclear RNA: conserved positions in central domain and helix I are essential during the first and second step of pre-mRNA splicing. *Proc. Natl Acad. Sci. USA* **91**, 903–907 (1994).
15. Sun, J. S. & Manley, J. L. A novel U2–U6 snRNA structure is necessary for mammalian mRNA splicing. *Genes Dev.* **9**, 843–854 (1995).
16. Fabrizio, P. & Abelson, J. Thiophosphates in yeast U6 snRNA specifically affect pre-mRNA splicing *in vitro*. *Nucleic Acids Res.* **20**, 3659–3664 (1992).
17. Yu, Y. T., Maroney, P. A., Darzynkiwicz, E. & Nilsen, T. W. U6 snRNA function in nuclear pre-mRNA splicing: a phosphorothioate interference analysis of the U6 phosphate backbone. *RNA* **1**, 46–54 (1995).
18. Collins, C. A. & Guthrie, C. Allele-specific genetic interactions between Prp8 and RNA active site residues suggest a function for Prp8 at the catalytic core of the spliceosome. *Genes Dev.* **13**, 1970–1982 (1999).
19. Siatecka, M., Reyes, J. L. & Konarska, M. M. Functional interactions of Prp8 with both splice sites at the spliceosomal catalytic center. *Genes Dev.* **13**, 1983–1993 (1999).
20. Tuschl, T., Sharp, P. A. & Bartel, D. P. Selection *in vitro* of novel ribozymes from a partially randomized U2 and U6 snRNA library. *EMBO J.* **17**, 2637–2650 (1998).
21. Tuschl, T., Sharp, P. A. & Bartel, D. P. A ribozyme selected from variants of U6 snRNA promotes 2',5'-branch formation. *RNA* **7**, 29–43 (2001).
22. Madhani, H. D. & Guthrie, C. Randomization-selection analysis of snRNAs *in vivo*: evidence for a tertiary interaction in the spliceosome. *Genes Dev.* **8**, 1071–1086 (1994).
23. Valadkhan, S. & Manley, J. L. A tertiary interaction detected in a human U2–U6 snRNA complex assembled *in vitro* resembles a genetically proven interaction in yeast. *RNA* **6**, 206–219 (2000).
24. Tarn, W. Y. & Steitz, J. A. Highly diverged U4 and U6 small nuclear RNAs required for splicing rare AT-AC introns. *Science* **273**, 1824–1832 (1996).
25. Tarn, W. Y. & Steitz, J. A. Pre-mRNA splicing: the discovery of a new spliceosome doubles the challenge. *Trends Biochem. Sci.* **22**, 132–137 (1997).
26. Gish, G. & Eckstein, F. DNA and RNA sequence determination based on phosphorothioate chemistry. *Science* **240**, 1520–1522 (1988).
27. Boudvillain, M. & Pyle, A. M. Defining functional groups, core structural features and inter-domain tertiary contacts essential for group II intron self-splicing: a NAIM analysis. *EMBO J.* **17**, 7091–7104 (1998).
28. Burn, A. J. & Cadogan, J. I. G. The reactivity of organophosphorus compounds. Part IX, the reaction of thionates with alkyl iodides. *J. Chem. Soc.* 5532–5541 (1961).
29. Saenger, W. *Principles of Nucleic Acid Structure* 116–126 (Springer, New York, 1984).
30. Query, C. C., Strobel, S. A. & Sharp, P. A. Three recognition events at the branch-site adenine. *EMBO J.* **15**, 1392–1402 (1996).
31. Query, C. C., Moore, M. J. & Sharp, P. A. Branch nucleophile selection in pre-mRNA splicing: evidence for the bulged duplex model. *Genes Dev.* **8**, 587–597 (1994).
32. Koole, L. H., Agback, P., Glemarec, C., Zhou, X.-X. & Chattopadhyaya, J. Solution structure of pentameric and heptameric branched-RNA modelling the lariat structure of group II or nuclear m-RNA introns studied by one- and two-dimensional NMR spectroscopy at 500 MHz. *Tetrahedron* **41**, 3183–3206 (1991).
33. Lehman, I. R. DNA ligase: structure, mechanism, and function. *Science* **186**, 790–797 (1974).
34. Yu, Y. T., Maroney, P. A. & Nilsen, T. W. Functional reconstitution of U6 snRNA in nematode *cis*- and *trans*-splicing: U6 can serve as both a branch acceptor and a 5' exon. *Cell* **75**, 1049–1059 (1993).
35. Tani, T. & Ohshima, Y. mRNA-type introns in U6 small nuclear RNA genes: implications for the catalysis in pre-mRNA splicing. *Genes Dev.* **5**, 1022–1031 (1991).
36. Huang, Z. & Szostak, J. W. A simple method for 3'-labeling of RNA. *Nucleic Acids Res.* **24**, 4360–4361 (1996).
37. Santoro, S. W. & Joyce, G. F. A general purpose RNA-cleaving DNA enzyme. *Proc. Natl Acad. Sci. USA* **94**, 4262–4266 (1997).

### Acknowledgements

We thank K. Ryan for advice and helpful discussions and insights, T. Nilsen for suggestions and comments on the manuscript, and A. Pyle for helpful discussions, advice and suggestions. We also thank G. Zubay, D. Herschlag, T. Tuschl, M. Konarska, G. Just, H. Lonnberg and F. Eckstein for discussions and advice on the chemistry of the reaction, and H. Robertson and D. Bartel for discussion and comments. We also thank P. Nouri for technical assistance. This work is supported by the NIH.

Correspondence and requests for materials should be addressed to J.L.M. (e-mail: jlm2@columbia.edu).